

INVITED PAPER

High-rate growth of $\text{YBa}_2\text{Cu}_3\text{O}_{7-x}$ thick films and thickness dependence of critical current density

W. Jo *

Department of Physics and Division of Nanosciences, Ewha Womans University, Seoul, Korea

Received 6 August 2004

$\text{YBa}_2\text{Cu}_3\text{O}_{7-x}$ 후막의 고속 증착과 임계 전류 밀도의 두께 의존성

조월렴*

Abstract

High-rate *in-situ* $\text{YBa}_2\text{Cu}_3\text{O}_{7-x}$ (YBCO) film growth was demonstrated by means of the electron beam co-evaporation. Even though our oxygen pressure is low, $\sim 5 \times 10^{-5}$ Torr, we can synthesize as-grown superconducting YBCO films at a deposition rate of around 10 nm/s. Relatively high temperatures of around 900 °C was necessary in this process so far, and it suggests that this temperature at a given oxygen activity allows a Ba-Cu-O liquid formation along with an YBCO epitaxy. Local critical current density shows a clear correlation with local resistivity. Homogeneous transport properties with a large critical current density ($4 \sim 5 \text{ MA/cm}^2$ at 77K, 0T) are observed in top faulted region while it is found that the bottom part carries little supercurrent with a large local resistivity. Therefore, it is possible that thickness dependence of critical current density is closely related with a topological variation of good superconducting paths and/or grains in the film bodies. The information derived from it may be useful in the characterization and optimization of superconducting films for electrical power and other applications.

Keywords : High-rate growth, $\text{YBa}_2\text{Cu}_3\text{O}_{7-x}$, thick film, electron beam co-evaporation, critical current density

I. Introduction

Our goal is to develop a process to grow *in-situ* superconducting $\text{YBa}_2\text{Cu}_3\text{O}_{7-x}$ (YBCO) films, directed towards coated conductor tape synthesis for electric power applications. The requirements are challenging due to the economic constraints:

deposition rate of greater than 10 nm/s and thickness of microns over large areas while preserving excellent superconducting properties. The electron beam co-evaporation method employed is promising in terms of relatively inexpensive material cost, easy wide-area expandability, and high-rate thick-film deposition. Here we report reproducible YBCO film fabrication with high superconducting critical current density ($J_c > 2 \text{ MA/cm}^2$) at around 10 nm/s of deposition rate on single crystal substrates as a preliminary demonstration for coated conductors.

*Corresponding author. Fax : +82 2 3277 2372
e-mail : wmjo@ewha.ac.kr

In addition, we report a simpler way to carry out depth profiling and extend its application to study the depth dependence of both the critical current density and the resistivity of a superconducting film. The essence of our approach is to use wet etching as simple and rapid means of depth profiling.

II. Experiment

Films were grown by means of molecular beam epitaxy (MBE) with electron beam co-evaporation of Y, Ba and Cu metal sources in oxygen atmosphere, or so-called reactive co-evaporation. Details are described elsewhere [1,2]. Y and Ba metal evaporation rates were controlled by laser atomic absorption sensors [3], and the Cu rate by chopped ion gauge monitor [2]. Molecular oxygen was introduced in two ways: into the growth chamber background generally, and alternatively by means of 1-inch diameter nozzle directed to the substrate surface to enhance the flux. A 500 W halogen-lamp-based radiation heater could heat the sample holder to 1000 °C. Most films were grown in a system background pressure of 5×10^{-5} Torr regardless of the nozzle or general chamber use, at oxygen flow rate of around 35 sccm for the general case, and 52 sccm for the nozzle case. Temperatures ranging from 860 to 1000 °C were explored in this report; a much wider range was used in developing the process.

Etching of the films was achieved using Bromine-methanol (0.1 vol %) [4]. This etching process is a well known method not to damage the remaining YBCO layers and has been used for a fabrication of Josephson junctions or in recovery experiments of deoxygenated YBCO materials. Critical currents of the films as a function of etching depth were measured using a Keithley 228A current source in a 0.5 T magnetic field applied perpendicular to the plane of the film.

III. Results and Discussion

X-ray diffraction (XRD) as well as resistivity-vs.-temperature (ρ -T) curves of films grown on LaAlO₃ (001) substrate indicates good epitaxy and electrical

properties, although small amounts of secondary phases, including BaCuO₂ ("011") and CuO are found (as expected from the decomposition of "012" as discussed later). Y₂O₃ is often observed as well. Samples were grown at deposition rates from 8.7 nm/s to 36 nm/s. In this paper we will focus on samples grown at 10 nm/s in 5 to 6.0×10^{-5} Torr of total pressure (mainly oxygen) with thickness around 0.5 to 1 μ m.

Figure 1 shows a summary of the reported thermodynamic stability diagram of YBCO along with our data superposed. YBCO is stable in the gray region. The upper-right (high-pressure) stability limit line is based on results of Williams's *et al.*[5] and Lindemer *et al.*[6] YBCO decomposes into Y₂BaCuO₅ ("211") and Ba₂Cu₃O₅ ("023") at the condition above the boundary line. The lower-left boundary is composed of three lines. The leftmost line is adopted from the work of Lindemer *et al.*[6] and shows that YBCO decomposes into "211" and Ba-Cu-O liquid (L) below the line, i.e. peritectic melting of YBCO. The other two lines are after MacManus-Driscoll [7]. The middle one stands for "211" + L decomposition boundary, the same as Lindemer's. Thus, these two lines are not necessarily discontinuous but connected with a certain curvature. The lowest segment (low pressure and temperature) line is for YBCO decomposition into "211", YBa₃Cu₂O₆ ("132" or "143"), and BaCu₂O₂ ("012"). This "012" phase is L if the temperature is higher than around 780~800 °C. It is however solid at the lower temperature, i.e. no L phase appears during YBCO decomposition.

Considering only the "012" material (i.e., pure BaCu₂O₂), which is around the eutectic melting composition of Ba-Cu-O [7,8], the "012" phase stability limit is superposed in Fig. 1 with a thick dashed line, as reported by MacManus-Driscoll [7]. We note that the eutectic composition actually changes as function of temperature and oxygen pressure, as described by Lindemer and Specht [8]. The "012" phase becomes unstable and decomposes into solids "011" and CuO as the temperature-pressure parameters crosses over the line. The "012" itself has two physical phases: L at higher temperature region, hatched in Fig. 1 and a solid at lower temperature and lower oxygen pressure region

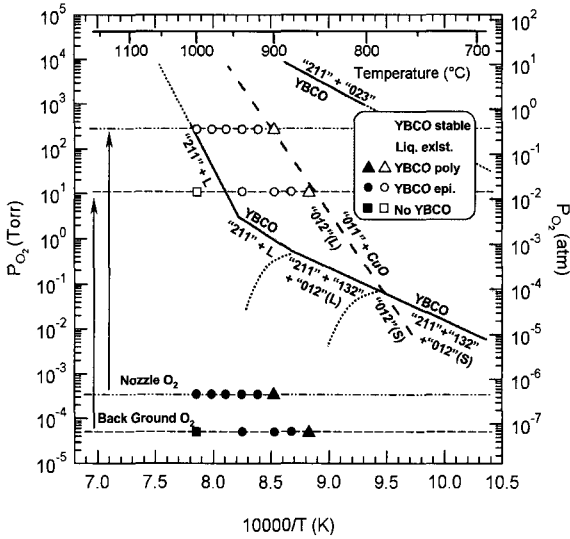


Fig. 1. Stability diagram for YBCO and "012". The area in gray denotes thermodynamically stable condition of YBCO. The "012" liquid phase exists in the hatched area and the thick dashed line is its boundary to decompose into solid "011" and CuO. Closed symbols indicate actual deposition conditions and open ones their re-plots in equivalent molecular oxygen pressure adjusted to fit the results to the stability limits. Extremely enhanced oxidation activity is considered caused by electron beam activated oxygen disassociation. Circles, triangles, and squares indicate YBCO epitaxial, polycrystalline, and no YBCO phase included films, respectively.

as indicated in Fig. 1. It appears that Y has little effect on this, as its solubility is less than 0.1 % in the liquid at the lower temperatures [9,10]. The L-solid phase transition point is on the intersection with the above-mentioned YBCO lower stability line [7].

A significant fact can be extracted from the construction of Fig. 1. Both YBCO and the "012" L phase coexist in an overlapping region as shown in Fig. 1, i.e. they are in equilibrium (see Fig. 2 and the discussion). It indicates that YBCO can be grown with the aid of the "012" L in this region, similar to liquid phase epitaxy (LPE) and is related to Tri-Phase-Epitaxy (TPE) reported by Yun *et al.*[11] using PLD at a rate of ~ 0.1 nm/sec, and oxygen pressure of 200 mTorr.

At low rates in the liquid region the growth is entirely 2D growth, as demonstrated in the Tri-Phase-Epitaxy work. Without the liquid, at lower

temperatures, the growth is island growth. This is the usual condition for YBCO film growth in the literature using PVD, with the nominal rate about 0.1 nm/s. The limiting rate at which ordered growth can be found is perhaps less than ~ 2 nm/s. Above that or some rate the growth is disordered. An exception is Pulsed Laser Deposition, for which the time between pulses allows ordering by surface diffusion.

Our growth condition seems very far from the YBCO stable condition in terms of oxygen pressure as plotted with closed symbols in the bottom of Fig. 1. The pressure used, $5\text{--}6 \times 10^{-5}$ Torr, is consistent with MBE-type condition, with a long mean free path (important for high rate and large area processing). With the use of the nozzle, the oxygen pressure at the substrates estimated from the oxygen flow rate and nozzle geometry is still extremely insufficient to form YBCO. We can, however, grow YBCO films with as-grown superconducting state, suggesting that the actual oxidation activity is much higher. In other words, some amount of activated oxygen species, e.g., possibly atomic oxygen, are involved. The source of these species is not yet known exactly, but we assume it takes place at the intensively electron beam irradiated metal sources interacting with molecular oxygen [1,2]. It is important to find and control this source and this is the goal for future research.

By taking account of the high oxidation activity, our growth conditions can be re-plotted as a molecular oxygen equivalent pressure according to the quality of YBCO films at various temperatures with/without nozzle use. Surprisingly, the results suggest that our equivalent oxygen pressure is more than 5 orders of magnitude higher than the measured values (Fig. 1, arrows). In assigning the data to a particular oxygen activity, we have neglected the stabilizing effect of the epitaxy energy of the growth on the substrate.

The average critical current densities $\langle J_c \rangle$ and the average conductivities at room temperature $\langle \sigma \rangle$ as a function of YBCO thickness of our *in-situ* electron-beam deposited YBCO films are shown in Fig. 2. The commonly observed decrease in $\langle J_c \rangle$ with thickness is evident. The thickness dependence of $\langle J_c \rangle$ and $\langle \sigma \rangle$ and has been observed in YBCO films on artificial metal tapes as well as on crystals regardless of the high quality of microstructure.

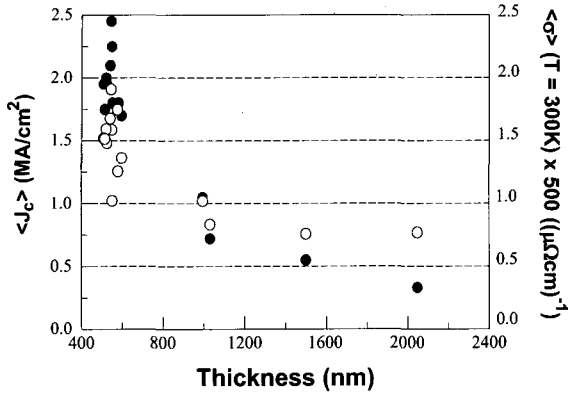


Fig. 2. Thickness dependence of average critical current density and average conductivity at 300K. Solid circles represent critical current density and open circles conductivity. Conductivity is scaled up by a factor of 500 to match the range with critical current density. As thickness of YBCO increases, the critical current density and conductivity decrease in the same manner, indicating that critical current density in the YBCO films are correlated to resistivity.

The same trend is observed in the average conductivities. From this coincidence, it is tempted to consider the correlation between critical current density and conductivity (or resistivity) of the YBCO films.

In Fig. 3, local critical current density, $J_c(z)$, of two samples as a function of etched layer number are shown: (a) initially 550nm-thick YBCO film and (b) initially 1050 nm-thick YBCO film. Each etched layer has different thickness, which was measured by a stylus profilometer. We note that the average zero-field critical current density of the film (a) before etching was 1.8 MA/cm² and the thick film (b) was 1.05 MA/cm². The values shown are obtained in $H = 0.5T$ and at $T = 77K$.

In Fig. 3(a), $J_c(z)$ shows two distinct regions. Top region shows high critical current density with uniform values, which have been observed by other groups. The $J_c(z)$ of this region is corresponding to 4 ~ 5 MA/cm² at $H = 0T$, $T = 77K$, which is promising for practical coated conductor applications. On the other hand, $J_c(z)$ drastically decreases in the bottom region as the film is thinned due to etching. Indeed, $J_c(z)$ goes to zero at a finite thickness of 200 nm (layers 7 – 10). Manifestly, this film has a

non-uniform distribution of critical current densities. The top part has a very local J_c while the bottom part has a vanishing J_c , different from the case of pulsed laser deposition (PLD) films reported by Foltyn *et al.* [13,14]. The bottom 'dead layer' in Ref. 13 is a non-superconducting layer with constant thickness regardless of total thickness. Its origin is proposed as a reaction between substrate and YBCO. Also, in the case of Ref. 13, the observed decrease in the average critical current density is attributed to the poor microstructure at the top regions of the film above the good YBCO layer in the middle. So, basically

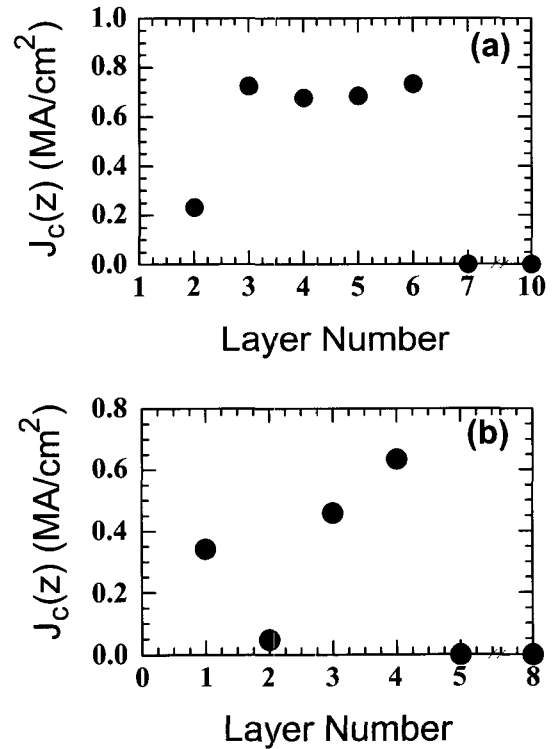


Fig. 3. (a) Local critical current density, $J_c(z)$, of the various layers of 550 nm-thick sample measured at $H = 0.5 T$. The symbols represent calculated local current density extracted from the average current density over the remaining thickness. (b) Local critical current density, $J_c(z)$, of the various layers of 1050 nm-thick sample measured at $H = 0.5 T$. The symbols represent calculated local current density extracted from the average current density over the total remaining thickness. Note that the kink at the 2nd layer is related to process control fluctuation in particular to Cu-flux wavering.

their PLD samples have three different layers. However, in our case, the 'bottom dead layer' tends to increase as the total thickness increases. It is the main reason for the decrease in the average $\langle J_c \rangle$ in the film (b). These results clearly illustrate various aspects of the mysteries of the thickness dependence of YBCO films J_c for coated conductors. Therefore, it is more desirable to study depth profiling of transport properties rather than simply to measure critical current density as a function of thickness.

The behavior illustrated here originated from the faulted island-growth type layers on the upper portions of our films and more perfect (but oxygen deficient) layer-by-layer grown layers on the lower portion, as revealed by transmission electron microscopy. This two-layer structure is in turn related to the process of growth in our approach, whose process is more akin to liquid phase epitaxy than traditional physical deposition. Our goal here is to dig deeper into what is going on and to demonstrate a practical way to quantify such effects.

As shown in Fig. 3(b), the thickness of the lower "dead-layer" is bigger than about 625 nm (layers 5 – 8). When the film thickness is increased, the layer-by-layer grown grains are bigger also increased proportionally. It is not clear why the layer-by-layer grown grains are getting thicker in our liquid-assisted growth of YBCO films. We need to understand more about thermodynamic relations between Ba-Cu-O and YBCO formation. Especially, it is critical to figure out the function of supersaturation, which is a control factor to extract YBCO phase from Ba-Cu-O melted flux. In addition, in this case we see considerable variation of the local J_c . In any events, we again see the value of depth profiling measurements, which will be used to trace back the deposition as well as microstructure and transport characterization. It would be difficult to understand and optimize our deposition process (and likely any process) without such information.

IV. Conclusion

Synthesis of the *in-situ* high J_c -YBCO film was demonstrated at a high deposition rate of around 10 nm/s using the electron beam evaporation at low pressure. The current deposition temperature is

high for coated conductor application due to chemical reaction with present buffer materials. However, lower temperature film growth down to 800 °C may be possible with lowering the oxidation activity. Additional lowering is expected by the lowering of the melting point of the Ba-Cu-O which has been shown with the addition of fluorine [15]. A high rate and large area process (owing to long mean free path) potentially can produce economical coated conductors [16]. Our results also demonstrate the complexities of the materials that lie under the observed failure of the critical current of coated conductors to scale linearly with thickness. Local critical current density shows a clear correlation with local resistivity. The large critical current density (4 ~ 5 MA/cm² at 77K, 0T) is promising for superconducting films for electrical power and other applications if we could optimize growth conditions in our liquid-assist high speed growth

Acknowledgements

This work is supported by ETEP through Korea Polytechnic University.

References

- [1] L.S.-J. Peng, W. Wang, W. Jo, T. Ohnishi, A.F. Marshall, R.H. Hammond, M.R. Beasley, and E.J. Peterson, IEEE Transactions on Applied Superconductivity **11**, 3375 (2001).
- [2] W. Jo, L.S.-J. Peng, W. Wang, T. Ohnishi, A.F. Marshall, R.H. Hammond, M.R. Beasley, and E.J. Peterson, J. Cryst. Growth **225**, 183 (2001).
- [3] W. Wang, R.H. Hammond, M.M. Fejer, and M.R. Beasley, J. Vac. Sci. Technol. **A17**, 2676 (1999).
- [4] W. Jo, T. Ohnishi, J. Huh, R. H. Hammond, and M. R. Beasley, IEEE Trans. Appl. Supercon. **13**, 2817 (2003).
- [5] R.K. Williams, K.B. Alexander, J. Brynstad, T.J. Henson, D.M. Kroeger, T.B. Lindemer, G.C. Marsh, J.O. Scarbrough, and E.D. Specht, J. Appl. Phys. **67**, 6934 (1990); R.K. Williams, K.B. Alexander, J. Brynstad, T.J. Henson, D.M. Kroeger, T.B. Lindemer, G.C. Marsh, J.O. Scarbrough, and E.D.

- Specht, *J. Appl. Phys.* **70**, 906 (1991).
- [6] T.B. Lindemer, F.A. Washburn, C.S. MacDougal, R. Feenstra and O.B. Cavin, *Physica* **C178**, 93 (1991).
- [7] J.L. MacManus-Driscoll, J.C. Bravman, and R.B. Beyers, *Physica* **C241**, 401 (1995).
- [8] T.B. Lindermer and E.D. Specht, *Physica* **C255**, 81 (1995).
- [9] W. Wong-Ng and L. P. Cook, *J. Res. NIST* **103**, 379 (1998).
- [10] Y. Shiohara and E. A. Goodilin, "Single Crystal Growth for Science and Technology." Review chapter in *Handbook on the Physics and Chemistry of Rare Earths*, edited by K. A. Gschneidner, Jr., L. Eyring, and M. B. Maple; Vol. 30, High Temperature Rare Earths Superconductors - I, Chapter 189, pp. 67-227 (2000).
- [11] K.S. Yun, B.D. Choi, Y. Matsumoto, J.H. Song, N. Kanda, T. Ito, M. Kawasaki, T. Chikyow, P. Ahmet, and H. Koinuma, *Appl. Phys. Lett.* **80**, 61-63 (2002).
- [12] B.T. Ahn, V.Y. Lee, R. Beyers, T.M. Gur, and R.A. Huggins, *Physica C* **167** (1990) 529-537, R. Beyers and B.T. Ahn, *Annu. Rev. Mater. Sci.* **21**, 335 (1991).
- [13] S. R. Foltyn, Q. X. Jia, P. N. Arendt, L. Kinder, Y. Fan, and J. F. Smith, *Appl. Phys. Lett.* **75**, 3692 (1999).
- [14] S. R. Foltyn, P. Tiwari, R. C. Dye, M. Q. Le, and X. D. Wu, *Appl. Phys. Lett.* **63**, 1848 (1993).
- [15] Wong-Ng, W., Cook, L.P., Suh, J., Levin, I., Vaudin, M., Feenstra, R., and Cline, J.P., in *Materials for High-Temperature Superconductor Technologies*, edited by M. P. Paranthaman, M. W. Rupich, K. Salama, J. Mannhart, T. Hasegawa. (Mater. Res. Soc. Symp. Proc. **689**, Warrendale, PA, 2002), p. 337.
- [16] R.H. Hammond, *Advances in Superconductivity VIII*, Proc. 8th Int. Symp. Supercond. (ISS) (Springer, Hamamatsu, 1996) 1029-1034.